ACS APPLIED MATERIALS & INTERFACES

Research Article

Cite This: ACS Appl. Mater. Interfaces 2019, 11, 42744−42750

www.acsami.org

A Lactate/Oxygen Biofuel Cell: The Coupled Lactate Oxidase Anode and PGM-Free Fe−N−C Cathode

Kunqi Wang,[†,‡] Lei Du,[‡] Qiliang Wei,[‡] Jihai Zhang,[‡] Gaixia Zhang,[‡] Wei Xing,*[,§] and Shuhui Sun*[,‡]

[†]Key Laboratory of Urban Sewage Treatment of Jilin Province, Department of Applied Chemistry, Changchun Institute of Technology, 130021, Changchun, China

[‡]Institut National de la Recherche Scientifique (INRS)-ÉnergieMatériaux et Télécommunications, Varennes, Québec J3 × 1S2, Canada

[§]State Key Laboratory of Electroanalytical Chemistry, Jilin Province Key Laboratory of Low Carbon Chemical Power, Changchun Institute of Applied Chemistry, Chinese Academy of Sciences, 130022 Changchun, China

Supporting Information

ABSTRACT: The rapid development of both wearable and implantable biofuel cells has triggered more and more attention on the lactate biofuel cell. The novel lactate/oxygen biofuel cell (L/O-BFC) with the direct electron transfer (DET)-type lactate oxidase (LOx) anode and the platinum group metal (PGM)-free Fe−N−C cathode is designed and constructed in this paper. In such a reasonable design, the surface-controlled direct two-electron electrochemical reaction of the lactate oxidase was determined by cyclic voltammetry (CV) on the carbon nanotube (CNT) modified electrode with favorable high electrochemical active surface area and electronic conductivity. Additionally, the biosensor based on DET-type LOx modified electrode impressively presented linear response to lactate with different concentrations from 0.000 mM to 12.300 mM. In particular, the apparent Michealis-constant (K_M^{app}) calculated as 0.140 mM clearly indicates that LOx on CNT has strong affinity to the substrate lactate. Meanwhile, 4e$^-$ transfer oxygen reduction reaction (ORR) was proven to take place on the Fe−N−C catalysts inthe 0.1 M PBS system, indicating the advantage by using the Fe−N−C catalysts at the cathode of L/O-BFC. Last but not least, the L/O-BFC with the direct electron transfer (DET)-type lactate oxidase(LOx) anode and the Fe−N−C cathode produced an superior open circuit potential (OCP) of 0.264 V and a maximum output power density (OPD) of 24.430 μW cm^{-2} in O_2 saturated 95.020 mM lactate solution. The above results will not only bring about significant interest in developing a DET-type biofuel cell, but also offer guiding direction to explore novel catalyst materials for the biofuel cell. This work enriches the research content and may push developments of the implantable and wearable biofuel cell forward.

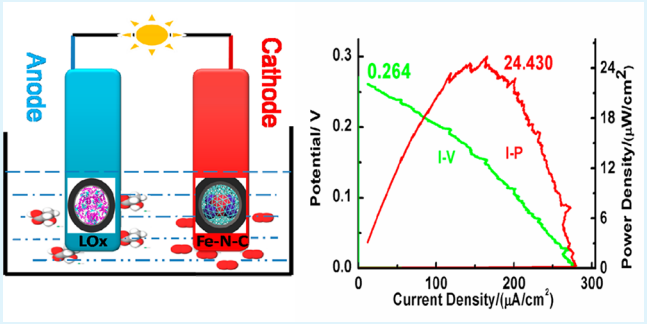

KEYWORDS: *lactate/oxygen biofuel cell, oxygen reduction reaction (ORR), direct electron transfer, lactate oxidase, Fe−N−C catalyst*

Downloaded via CARLETON UNIV on July 13, 2020 at 05:42:07 (UTC).
See https://pubs.acs.org/sharingguidelines for options on how to legitimately share published articles.

1. INTRODUCTION

Biofuel cells (BFCs) consist of two primary types: one is an enzyme biofuel cell,[1] and the other one is a microbial fuel cell,[2−4] both of which are typical energy conversion devices that consume renewable biofuels to generate clean electrical energy. The enzyme biofuel cell has been emerging as a promising power source for implantable biomedical electronic and wearable microelectronic devices.[5,6] Among various enzyme biofuel cells, that with anodic lactate oxidation reaction and cathodic oxygen reduction reaction, that is, a lactate/oxygen biofuel cell (denoted as L/O-BFCs), is promising and attracts extensive attention due to the high energy feature and abundant resource of lactate[7,8] For example, a particular L/O-BFC with 70.000 mW cm^{-2} in output power density was successfully implanted in the human arm,[9] and wearable L/O-BFCs were integrated into headbands to light a blue LED.[10]

At anode of L/O-BFC, the lactate is oxidized to pyruvate, which is accelerated by lactate oxidase or lactate dehydrogenase catalysis; whereas ORR occurs on the cathode. Based on such principles, L/O-BFCs are subjected to challenging DET between lactalase and the electrode, and the sluggish ORR. In this regard, the L/O-BFCs are require improvement in terms of efficiency, current and power density, and stability, etc.[1] This report strives to achieve high-performance L/O-BFCs by reasonably coupling DET lactalase, particularly lactate oxidase anode and efficient cathode.

Received: August 13, 2019
Accepted: October 22, 2019
Published: October 22, 2019

© 2019 American Chemical Society

DOI: 10.1021/acsami.9b14486
ACS Appl. Mater. Interfaces 2019, 11, 42744−42750

So far, DET of lactate dehydrogenase has been achieved on Au electrode,[11] a carbon screen printed electrode,[12] a glassy carbon electrode,[13] and polyaniline films electrode, etc.[14] However, DET of lactate oxidase has been rarely touched. The lactate oxidase extracted from bacteria is usually 5.000 nm spherical flavoprotein, and the FNM/$FNMH_2$ active center is embedded inside.[15,16]

In order to realize the DET between enzyme catalyst and electrode, one of the most effective methods is to improve the number of enzyme catalysts at certain geometric surfaces by building nanometer pores and micrometer holes on the electrode surface with carbon and gold nanomaterial;[17] another way is to optimize electronic connections between the enzyme and electrode interface using nanomaterials with adequate porosity/dimensions by tailoring orientation of an enzyme catalyst with the help of a chemical force (such as hydrophobic interactions, electrostatic interactions, and covalent bonding, etc.).[18] In a word, nanomaterial potentially plays an important role during the DET between enzyme catalyst and electrode.

Carbon nanotubes (CNTs) are attractive as electrodes due to their good conductivity, considerable mechanical strength, high electrochemical active surface area, alleviation of surface fouling, and capability to be functionalized.[19−21] In biofuel cell and biosensor research, CNTs can potentially promote DET between the active center of enzyme and electrode surface and help the enzyme to perform complete direct electrochemical processes.[22] Indeed, scientists have discovered and reported the DET of multiple enzymes on CNT modified electrodes.[23,24] Therefore, it is not surprising that lactate oxidase biosensor with CNT modified electrodes can be constructed successfully.[25,26] In addition, the biocompatibility of electrode materials is especially important for implantable bioelectronic devices. It is reported continuously that CNT is an ideal biocompatible material.[27−29] In 2013, the power density of L/O-BFC based on a CNT modified electrode was reported up to 70 μW cm^{-2}.[9] Therefore, it will be a very wise choice to employ CNT modified electrodes in future L/O-BFC.

In addition to the anode, efficient ORR catalysts at the cathode is urgently needed to get an applicable L/O-BFC system. Pt-based catalyst[7,12] and enzyme-based catalysts[30−32] have been investigated as cathode catalysts in BFCs. For example, the maximum OPD of L/O-BFC exceeds 20.000 μW cm^{-2} by employing Pt-based catalysts at the cathode.[12]

However, Pt-based catalyst is too costly to be widely applied in the L/O-BFCs. To replace Pt-based ORR catalysts in BFCs, various catalysts have been developed and prepared with three primary directions: (i) metallic complexes with nitrogen-containing moieties; (ii) transition metal oxides; and (iii) biocatalysts.[33] Among these, Fe−N−C catalysts have attracted much attention due to their excellent activity, low price, and high durability.[34−36] The Fe−N−C catalysts are rarely employed in enzymatic biofuel cells, in contrast to the extensive investigations in PEM fuel cell systems.[37−39]

Herein, a novel and effective L/O-BFC is established by coupling lactate oxidation and ORR at the anode and cathode in 0.1 M PBS media, which presents up to 24.430 μW cm^{-2} in power output, superior to previous reports, such as ref 12. This superior performance can be attributed to both the DET behavior of lactate oxidation on the lactate oxidase-modified-CNT electrode and the advanced Fe−N−C catalysts with efficient ORR processes.

2. MATERIALS AND METHODS

2.1. Chemicals. Lactate oxidase (LOx, L9795−50UN, Aerococcus viridians), Lithium lactate (440469−50g), and 5 wt % Nafion solution were obtained from Sigma-Aldrich. CNTs were purchased from Baytubes MIV-05-182 (Bayer AG). Sodium phosphate (S-373) and sodium phosphate monobasic (S-369) were obtained from Fisher Scientific Company. All the chemical reagents were not purified before using.

2.2. Catalyst and Electrode for Electrochemical Tests. *Fe−N−C catalysts.* Fe−N−C catalyst was prepared according to our previous report.[40] The detailed physical characterizations of Fe−N−C catalyst were provided in ref 40. Figure 1 demonstrates the structure of catalyst.

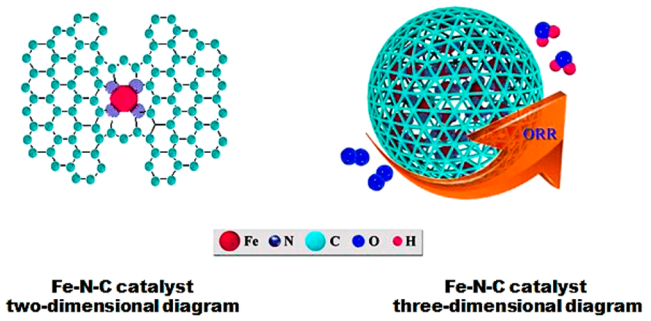

Figure 1. A structure illustration of the Fe−N−C catalyst.

Electrochemical Characterizations. In a conventional three-electrode system, all electrochemical tests were completed. The glassy-carbon rotating disk electrode (5.000 mm in diameter, RDE, PINE Research Instrumentation) and/or rotating ring-disk electrode (RRDE) with Pt ring and glassy-carbon disk (5.610 mm in diameter) were the working electrode, whereas a Ag/AgCl electrode and a Pt wire were the reference and counter electrode, respectively. Before use, first, the glassy carbon electrodes in RDE/RRDE were cleaned by ultrasound in an aqueous solution and subsequently polished. The electrolyte solution used in this report was phosphate buffer solution (PBS, 0.1 M). The details for electrode preparation are presented below.

Fe−N−C/GC Electrode. First, 1.200 mg of Fe−N−C catalyst was dispersed in a mixed solvent with 20.000 μL of 5.000 wt % Nafion solution and 70.000 μL of ethanol by alternate sonication and agitation. Then, 11.000 μL of the Fe−N−C catalyst dispersion liquid was dropped onto the GC electrode surface (the loading of catalyst is about 0.730 mg cm^{-2}), and finally dried in air. The Fe−N−C/GC electrodes were used for ORR test in fresh 0.1 M PBS (pH 7.0).

Nafion/LOx/CNT/GC Electrode. A homogeneous CNTs suspension was prepared by dispersing 2.000 mg CNTs into 1.000 mL of ethanol. At the same time, 0.130 UN μL^{-1} of LOx solution was obtained by dissolving 0.66 mg of solid LOx powder into 300.000 μL 0.1 M PBS (pH7.0). Then, 10 μL of the CNT/ethanol suspension was covered on the 5.000 mm diameter GC RDE and dried at room temperature for 20 min to form a CNT thin film. After that, 10.000 μL of the 0.130 UN μL^{-1} LOx solution was dropped on the CNT thin film to form a hybrid LOx/CNT film electrode. The LOx/CNT electrode was protected by dropping 2.000 μL of 5.000 wt % Nafion solution before testing. Such an electrode was denoted as Nafion/LOx/CNT/GC electrode. As referential electrodes, CNT/GC and Nafion/GC electrodes were formed in a similar way. The Nafion/LOx/CNT/GC electrode was placed in refrigerator to maintain the bioactivity.

2.3. Fabrication of Lactate Biosensor. First, 20.000 μL of CNT-ethanol solution (2.000 mg mL^{-1}), 10.000 μL of Nafion solution (5.000 wt %), and 20.000 μL of LOx solution (0.299 UN μL^{-1} PBS) were mixed in a 0.200 mL centrifuge tube, which was put in ultrasonic generator for 2 h of continuous ultrasound. Second, 12.000 μL of ultrasound mixed solution was dropped on the surface of glassy carbon electrode, and dried for 20 min at room temperature.

DOI: 10.1021/acsami.9b14486
ACS Appl. Mater. Interfaces 2019, 11, 42744−42750

Third, the electrode was used as working electrode during the lactate electrochemical oxidation.

2.4. Assembly of L/O-BFC. A lactate/oxygen biofuel cell coupled DET lactate oxidase anode and Fe−N−C cathode was assembled in a 50.000 mL beaker loaded with 0.1 M PBS or different concentration lactate solutions (shown in Figure 2). The anode of the L/O-BFC was

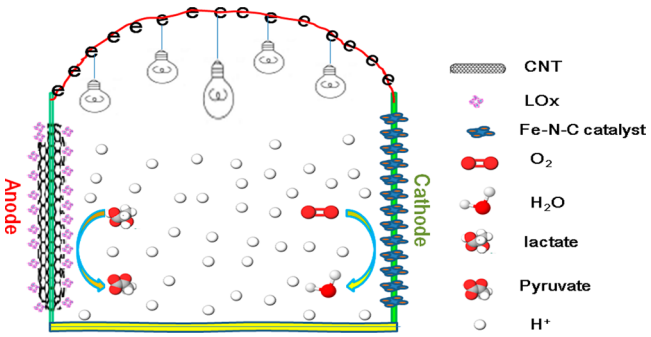

Figure 2. L/O-BFC structure diagram.

fabricated as following: 10.000 μL CNT-ethanol mixture solution (2.000 mg CNT mL^{-1}), 10.000 μL LOx (0.299 UN μL^{-1}) solution, and 5.000 μL Nafion solution (5.000 wt %) was drop-cast orderly on a 0.196 cm^2 round carbon paper, which was pressed tightly on one end of a nickel foam (60.000 mm long and 8.000 mm wide), Next, 1.000 mg of Fe−N−C catalyst was mixed with 70.000 μL of ethanol solution and 20.000 μL of Nafion solution(5.000 wt %) in a glass vial under sonication for 1 h. Following similar procedures, 10.000 μL of mixed solution including Fe−N−C catalyst was drop-cast on a 0.196 cm^2 round carbon paper surface, which was pressed upon the foamed nickel, so the cathode of the L/O-BFC based Fe−N−C catalyst was structured completely. At normal temperatures and pressures, the performance parameters of the L/O-BFC were read and recorded by using a BioLogic SP-150 Potentiostat with a VMP3B-20 Booster driven by an EC-Lab V9.98.

3. RESULTS AND DISCUSSION

3.1. The DET on Nafion/LOx/CNT/GC Electrode. As shown in SI Figure S1, the cyclic voltammogram (CV) curve c of the Nafion/LOx/CNT/GC electrode obviously shows redox peaks in 0.1 M PBS (pH 7.0) with 100 mV s^{-1} scan rate and potential windows from −0.800 to 0.800 V, in contrast to the CNT/GC electrode (curve b) and Nafion/GC electrode (curve a). The anodic and cathodic peak potentials of the Nafion/LOx/CNT/GC electrode locate at −0.343 V and −0.358 V, respectively, with a difference ΔEp of 0.015 V. The calculation value of formal potential ($E^{\circ\prime}$) of the Nafion/LOx/CNT/GC electrodes is −0.351 V, which is close to the formal potential of the flavodoxin at pH 7.0.[41] Moreover, the anodic peak current is slightly less than the cathodic peak current. Therefore, LOx immobilized on Nafion/LOx/CNT/GC electrodes can give rise to a direct reversible electrochemical reaction. The CNTs play a positive role to facilitate the DET of LOx.[23] In order to study the detailed electrochemical characteristics, CV curves of the Nafion/LOx/CNT/GC electrode at various scan rates (20, 40, 60, 80, 100, 120, 140, 160, 180, and 200 mV s^{-1}) were performed in 0.1 M PBS (Figure 3A). As the scan rate increases, the anodic peak potential moves to the positive direction while the cathodic peak potential moves to the negative direction. The cathodic and anodic peak current is linearly related to scan rate (fitting results: Pa: $Y = -6.579 \times 10^{-6} + 2.679 \times 10^{-4}X$, $R = 0.992$; Pc: $Y = -2.412 \times 10^{-6} - 2.544 \times 10^{-4}X$, $R = -0.991$), as shown in Figure 3B. Such linear relationships indicate that the

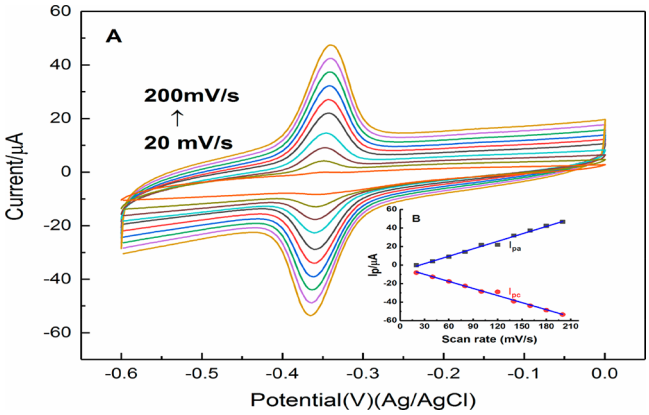

Figure 3. A CVs of the Nafion/LOx/CNT/GC electrode in 0.1 M pH 7.0 PBS (with different scan rate. The scan rate was 20, 40, 60, 80, 100, 120, 140, 160, 180, and 200 mV s^{-1}, respectively, (from inside to outside). Inset B: plotting peak current vs scan rate.

electrochemical behavior of LOx is a surface-controlled electrochemical process.[42] In this process, the number of electron transfer of the LOx is calculated as 2 according to equation FWHM $= \frac{90.6}{n}$.[43] Meanwhile, by combining equation $K_{ET} = \frac{\alpha n F v_c}{RT} = (1-\alpha)\frac{nFv_a}{RT}$ where $\alpha = 0.5$[43] based on the information on above cyclic voltammograms, the electron transfer rate constant (k_{ET}) is calculated as 0.956 s^{-1}. The surface coverage (Γ) of LOx on the Nafion/LOx/CNT/GC electrode is calculated as 2.950×10^{-10} mol cm^{-2} by the following equation $I_p = \frac{n^2F^2A\Gamma v}{4RT}$,[44] which is almost 2 orders of magnitude higher than the surface coverage (about 2.200×10^{-12} mol cm^{-2}) of LOx on both bare-gold or DTSP-gold electrode.[45] The above analysis demonstrates that the surface-controlled and reversible direct electrochemical process of LOx immobilized on Nafion/LOx/CNT/GC electrode is accompanied by two electrons (2e$^-$) transfer, and CNTs not only demonstrate huge superficial area but also give a suitable microenvironment for installing LOx onto glassy carbon electrode surface.

3.2. Biosensor Response of the LOx Electrode to Lactate. The relationship between electrochemical responses current of the LOx electrode and the lactate concentration was exhibited by cyclic voltammetry under oxygen saturated condition. In Figure 4A, as lactate concentration is increased from 0.000 mM to 9.000 mM, the peak current of O_2 reduction reaction decreases from 9.399×10^{-5} A to 8.615×10^{-5} A gradually. In other words, with the supply of lactate, a lactate oxidation reaction happens gradually. The electrons and protons for FMN reduction are provided by the lactate oxidation reaction. At the same time, some electrons and protons consumed in oxygen reduction come from $FMNH_2$ oxidation reaction. Thus, the oxidation peak of the oxidation reaction of the FMN disappears. The peak current response of the LOx electrode to different lactate concentration was displayed in Inset B of Figure 4. When lactate concentration was gradually increased from 0.000 mM to 12.300 mM, the peak current of the LOx electrode decreased linearly and its linear correlation coefficient is 0.941, its under signal-to-noise ratio is 3, and the detection limit is 0.376 mM. The responding sensitivity of LOx electrode is 0.749 mA M^{-1} which is much higher than 0.537 ± 0.007 mA M^{-1} produced by amucin/albumin hydrogel matrix/Nafion polymer lactate oxidase

DOI: 10.1021/acsami.9b14486
ACS Appl. Mater. Interfaces 2019, 11, 42744−42750

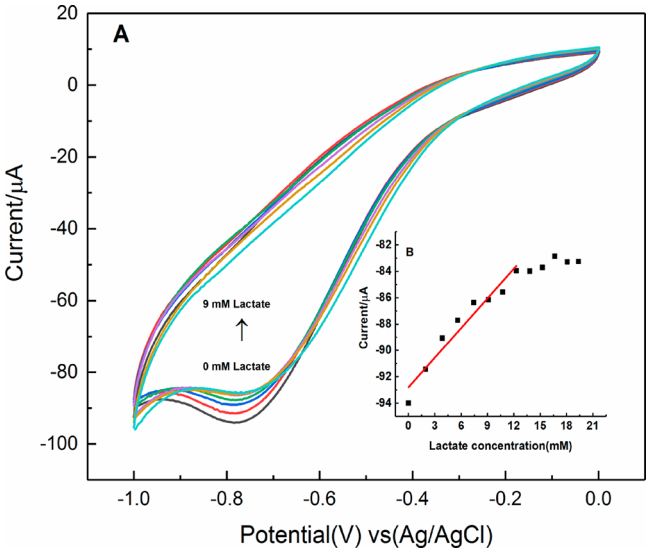

Figure 4. Relationship graph between electrochemical response current of the LOx electrode and different concentration lactate Figure. 4A, CVs of the LOx electrode in 0.000−9.000 mM lactate solution (from outer to inner) with 60 mV s^{-1} scan rate. Inset B, plotting response peak current of the LOx electrode to 0.000−20.000 mM lactate.

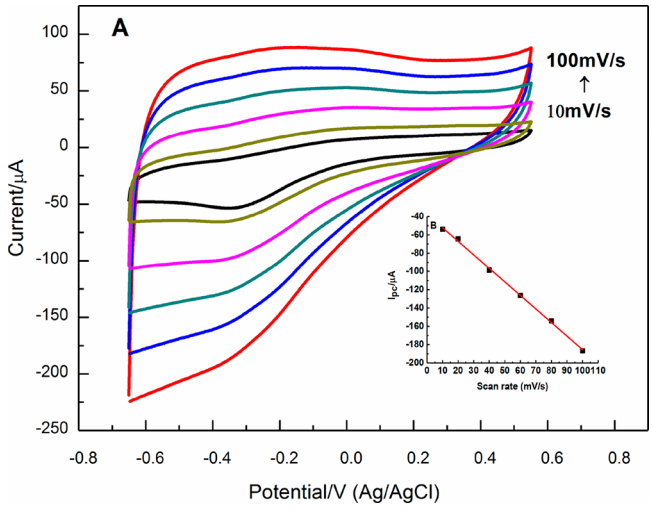

Figure 5. (A) The CVs of Fe−N−C/GC electrode in 0.1 M PBS (pH 7.0) buffer solution saturated with oxygen, scan rate: 10, 20, 40, 60, 80, and 100 mV/s, respectively (from inside to outside). Inset B, plotting ORR peak current of the Fe−N−C/GC electrode vs scan rate.

biosensor.[46] In addition, when lactate concentration is increased from 12.500 mM to 20.000 mM, the variation of peak current value is not obvious, which is due to the Michaelis−Menten kinetic reaction mechanism. Thus, based on Lineweaver−Burk equation,[47] the apparent Michealis-constant (K_M^{app}) was 0.140 mM, which was lower than 0.270 mM reported on gold electrode modified with LOx and dithiobis-*N*-succinimidyl.[48] Such small K_M^{app} value means that the LOx rooted in CNTs possessed higher enzymatic reaction activity and stronger affinity to lactate. Therefore, the LOx immobilized on CNT electrode in our case has presented good electrocatalytic response to O_2 and biosensor response to lactate. The experimental results indicate that CNT is a proper matrix material to immobilize LOx.

3.3. ORR Performance of the Fe−N−C/GC Electrode. The Fe−N−C/GC electrode was the working electrode in following ORR measurements. In 0.1 M pH 7.0 PBS solution saturated with O_2, the CVs under various scan rates are shown in Figure 5A. In Figure 5A, at 10 mV s^{-1}, the initial potential and peak potential of ORR locate at 0.130 V and −0.340 V, respectively. As the scan rate increased to 100 mV s^{-1}, the ORR peak potential showed nearly no changes, whereas the ORR peak current increased. From Figure 5B, in 0.1 M pH 7.0 PBS solution, the ORR peak current (I_{pc}) was linear with respect to scan rate (v) ($Y = -37.540-1480.450X$, $R = 0.999$), which indicates that the electrochemical reduction of oxygen catalyzed by Fe−N−C catalyst was a surface-controlled process. On the other hand, for calculating the electron transfer number and the productivity of peroxide in the above ORR electrochemical process, a linear sweep voltammograms (LSV) of the Fe−N−C/GC electrode were conducted in 0.1 M PBS solution saturated with O_2 (SI Figure S2). By combining with the equation reported in ref 40., electron transfer number was 4 and the productivity of peroxide was calculated as 2.744%. All electrochemical characteristic based on the Fe−N−C/GC electrode to ORR in 0.1 M PBS buffer solution proves that Fe−N−C is an efficient cathode catalyst in biofuel cells.

3.4. Evaluation of the L/O-BFC. The anode half reaction, the cathode half reaction and single cell reaction of the L/O-BFC based on DET-type LOx anode and Fe−N−C cathode are displayed in eqs 1−3. First, electrochemical oxidation reaction of lactate takes place on the anode: lactate reacts with oxygen and LOx/($FMNH_2$) to yield pyruvate, hydrogen peroxide, and LOx/(FMN), the half-wave potential of which was −0.081 V vs SHE (as shown in eq 1). Second, electrochemical reduction reaction of oxygen to water on the cathode happens at the half-wave potential of 0.140 V vs SHE (as shown in eq 2). Overall, the single cell reaction is shown as eq 3, and the open circuit potential of the L/O-BFC on the basis of DET-type LOx anode and Fe−N−C cathode is about 0.221 V. Subsequently, in the following three cases: (i) nitrogen saturated 0.1 M PBS buffer solution, (ii) oxygen saturated 0.1 M PBS buffer solution, and (iii) oxygen saturated different concentration of lactate solution, the performance of the L/O-BFC based on DET-type LOx anode and Fe−N−C cathode was given

Anode

$$\text{lactate} + O_2 + \text{LOx/(FMNH}_2) \rightarrow \text{pyruvate} + H_2O_2 + \text{LOx/FMN } E^a_{1/2} = -0.081\text{V vs. SHE} \quad (1)$$

Cathode

$$O_2 + 4H^+ + 4e^- \xrightarrow{\text{Fe-N-C}} 2H_2O\ E^c_{1/2} = 0.140\text{V vs SHE} \quad (2)$$

Biofuel cell

$$\text{lactate} + 2O_2 + 3\text{LOx/FMN H}_2 \rightarrow \text{pyruvate} + 2H_2O + H_2O_2 + 3\text{LOx/FMN}E^c_{1/2} - E^a_{1/2} = 0.221\text{vsSHE} \quad (3)$$

The polarization curves and the detailed performance data at each testing condition are shown in Figure 6 and Table.1, respectively. In nitrogen saturated 0.1 M PBS buffer solution, the OCP and the maximum OPD of the L/O-BFC was 0.130 V (dark gray curve a_1) and 3.000 μWcm^{-2} (dark gray curve a_2), respectively. In oxygen saturated 0.1 M PBS buffer solution, the OCP and the maximum OPD of the L/O-BFC increased

DOI: 10.1021/acsami.9b14486
ACS Appl. Mater. Interfaces 2019, 11, 42744−42750

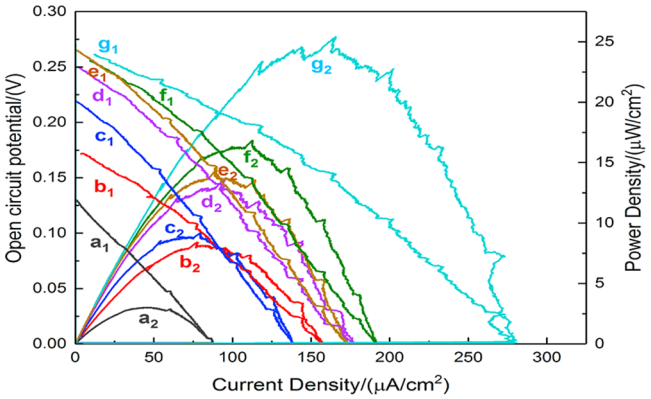

Figure 6. Polarization curves of the L/O-BFC in different concentration lactate solution saturated with N_2 or O_2, 0.000 mM lactate saturated with N_2(a_1, a_2 dark gray curve), 0.000 mM (b_1,b_2 red curve), 4.970 mM (c_1, c_2 oxford blue curve), 14.780 mM (f_1, f_2 green curve), 33.820 mM (d_1, d_2 purple curve), 61.030 mM (e_1, e_2 yellow curve) and 95.020 mM (g_1,g_2 light blue curve) lactate saturated with O_2, respectively.

Table 1. Performance Parameter of the L/O-BFC

lactate/mM	OCP (V)	OPD (μW cm^{-2})
0.000 (saturated N_2)	0.130	3.000
0.000 (saturated O_2)	0.171	8.110
4.970 (saturated O_2)	0.207	8.805
14.780 (saturated O_2)	0.253	16.275
33.820 (saturated O_2)	0.250	12.732
61.030 (saturated O_2)	0.262	13.600
95.020 (saturated O_2)	0.264	24.430

to 0.171 V (red curve b_1) and 8.110 μW cm^{-2} (red curve b_2), respectively. Then, when 4.970 (oxford blue curve), 14.780 (green curve), 33.820 (purple curve), 61.030 (yellow curve), and 95.020 mM (light blue curve) lactate solutions were saturated with O_2, the OCP and the maximum OPD of the L/O-BFC also increased gradually to 0.264 V and 24.430 μW cm^{-2}, respectively. All these results indicated that the L/O-BFC based on DET-type LOx and Fe−N−C cathode have been activated successfully. After a month, the OCP and the OPD of the L/O-BFC were retested in 4.970 mM lactate solution saturated with O_2 to evaluate the stability. The value of the OCP slightly decreased from 0.207 to 0.197 V, while the OPD decreased from 8.805 μW cm^{-2} to 7.880 μW cm^{-2}, exhibiting the higher stability of the L/O-BFC.

4. CONCLUSION

A direct reversible surface-controlled electrochemical process with two-electron transfer of the LOx was successfully realized on a CNT modified electrode. A highly sensitive lactate electrochemistry biosensor on the basis of the Nafion/LOx/CNT/GC electrode was constructed, exhibiting typical Michaelis−Menten kinetic characters. The catalyst Fe−N−C showed higher ORR performance in 0.1 M PBS buffer system. Accordingly, a unique L/O-BFC with DET-type LOx anode and Fe−N−C cathode was assembled When lactate concentration reached 95.020 mM, the OCP and the maximum OPD of L/O-BFC was 0.264 V and 24.430 μW cm^{-2}, respectively. This work is important to both (i) the direct electrochemical reaction of the LOx on modified electrode of carbon nanomaterials and (ii) the construction of DET-type lactate biosensor and DET-type lactate biofuel cell. This study also provides new thoughts and trends to apply Fe−N−C and nonenzyme catalyst as the air cathode of the biofuel cells. Our future work will focus on increasing the performances of the DET-type lactate biofuel cell based on Fe−N−C cathode catalyst, developing the implantable or wearable biofuel cell on the basis of the DET-type LOx anode and the Fe−N−C cathode.

■ ASSOCIATED CONTENT

Supporting Information

The Supporting Information is available free of charge on the ACS Publications website at DOI: 10.1021/acsami.9b14486.

Figure S1, the CVs of the Nafion/GC (a), CNT/GC (b), and Nafion/LOx/CNT/GC electrodes (c) in 0.1 M PBS (pH7.0), with 100 mV s^{-1} scan rate; Figure S2, the linear sweep voltammograms (LSV) of the Fe−N−C/GC electrode in 0.1 M pH 7.0 oxygen saturated PBS buffer solution (PDF)

■ AUTHOR INFORMATION

Corresponding Authors

*(W.X) E-mail: xingwei@ciac.ac.cn.
*(S.S) E-mail: shuhui@emt.inrs.ca.

ORCID

Shuhui Sun: 0000-0002-0508-2944

Author Contributions

The manuscript was written through contributions of all authors. All authors have given approval to the final version of the manuscript.

Notes

The authors declare no competing financial interest.

■ ACKNOWLEDGMENTS

The work is supported financially by China Scholarship Council (CSC) (File No: 201408220073) and supported by seed fund of Changchun Institute of Technology (No: 320190007), Discovery Grants from the Natural Sciences and Engineering Research Council of Canada (NSERC), Institut National de la Recherche Scientifique (INRS). L.D. acknowledges the scholarship under the International Post-doctoral Exchange Fellowship Program by the Office of China Postdoctoral Council (Grant No. 20180072), and the Fonds de Recherche du Québec—Nature et Technologies for Postdoctoral scholarship (V2, file number: 274384) in Quebec Canada.

■ REFERENCES

(1) Rasmussen, M.; Abdellaoui, S.; Minteer, S. D. Enzymatic Biofuel Cells: 30 Years of Critical Advancements. *Biosens. Bioelectron.* **2016**, *76*, 91−102.

(2) Zhao, C.; Wu, J.; Kjelleberg, S.; SayCheyLoo, J.; Zhang, Q. Employing a Flexible and Low-cost Polypyrrole Nanotube Membrane as an Anode to Enhance Current Generation in Microbial Fuel Cells. *Small* **2015**, *11*, 3440−3443.

(3) Song, R.; Wu, Y.; Lin, Z.; Xie, J.; Tan, C. H.; SayCheyLoo, J.; Cao, B.; Zhang, J.; Zhu, J.; Zhang, Q. Living and Conducting: Coating Individual Bacterial Cells with in situ Formed Polypyrrole. *Angew. Chem., Int. Ed.* **2017**, *56*, 10516−10520.

(4) Wang, V. B.; Du, J.; Chen, X.; Thomas, A. W.; Kirchhofer, N. D.; Garner, L. E.; Maw, M. T.; Poh, W. H.; Hinks, J.; Wuertz, S.; Kjelleberg, S.; Zhang, Q.; SayCheyLoo, J.; Bazan, G. C. Improving

DOI: 10.1021/acsami.9b14486
ACS Appl. Mater. Interfaces 2019, 11, 42744−42750

Charge Collection in Escherichia coli−carbon Electrode Devices with Conjugated Oligoelectrolytes. *Phys. Chem. Chem. Phys.* **2013**, *15*, 5867−5872.
(5) Campbell, A. S.; Jeong, Y. J.; Geier, S. M.; Koepsel, R. R.; Russell, A. J.; Islam, M. F. Membrane/Mediator-Free Rechargeable Enzymatic Biofuel Cell Utilizing Graphene/Single-Wall Carbon Nanotube Cogel Electrodes. *ACS Appl. Mater. Interfaces* **2015**, *7*, 4056−4065.
(6) Prasad, K. P.; Chen, Y.; Chen, P. Three-Dimensional Graphene-Carbon Nanotube Hybrid for High-Performance Enzymatic Biofuel Cells. *ACS Appl. Mater. Interfaces* **2014**, *6*, 3387−3393.
(7) Sokic-Lazic, D.; Andrade, A. R.; Minteer, S. D. Utilization of Enzyme Cascades for Complete Oxidation of Lactate in an Enzymatic Biofuel Cell. *Electrochim. Acta* **2011**, *56*, 10772−10775.
(8) Escalona-Villalpando, R. A.; Reid, R. C.; Milton, R. D.; Arriaga, L. G.; Minteer, S. D.; Ledesma-García, J. Improving the Performance of Lactate/Oxygen Biofuel Cells Using a Microfluidic Design. *J. Power Sources* **2017**, *342*, 546−552.
(9) Wenzhao, J.; Gabriela, V.; AmayJ, B.; JoshuaR, W.; Joseph, W. Epidermal Biofuel Cells: Energy Harvesting from Human Perspiration. *Angew. Chem., Int. Ed.* **2013**, *52*, 7233−7236.
(10) Jia, W.; Wang, X.; Imani, S.; Bandodkar, A. J.; Ramirez, J.; Mercier, P. P.; Wang, J. Wearable Textile Biofuel Cells for Powering Electronics. *J. Mater. Chem. A* **2014**, *2*, 18184−18189.
(11) Narwal, V.; Sharma, M.; Rani, S.; Pundir, C. S. An Ultrasensitive Amperometric Determination of Lactate by Lactate Dehydrogenase Nanoparticles Immobilized onto Au Electrode. *Int. J. Biol. Macromol.* **2018**, *115*, 767−775.
(12) Treu, B. L.; Minteer, S. D. Isolation and Purification of PQQ-Dependent Lactate Dehydrogenase from Gluconobacter and Use for Direct Electron Transfer at Carbon and Gold Electrodes. *Bioelectrochemistry* **2008**, *74*, 73−77.
(13) Nesakumar, N.; Sethuraman, S.; Krishnan, U. M.; Rayappan, J. B. B. Fabrication of Lactate Biosensor Based on Lactate Dehydrogenase Immobilized on Cerium Oxide Nanoparticles. *J. Colloid Interface Sci.* **2013**, *410*, 158−164.
(14) Chaubey, A.; Pande, K. K.; Singh, V. S.; Malhotra, B. D. Co-Immobilization of Lactate Oxidase and Lactate Dehydrogenase on Conducting Polyaniline Films. *Anal. Chim. Acta* **2000**, *407*, 97−103.
(15) Rassaei, L.; Olthuis, W.; Tsujimura, S.; Sudhölter, E. J. R.; Berg, A. Lactate Biosensors: Current Status and Outlook. *Anal. Bioanal. Chem.* **2014**, *406*, 123−137.
(16) Kaneko, H.; Minagawa, H.; Shimada, J. Rational Design of Thermostable Lactate Oxidase by Analyzing Quaternary Structure and Prevention of Deamidation. *Biotechnol. Lett.* **2005**, *27*, 1777−1784.
(17) Kwon, C. H.; Ko, Y.; Shin, D.; Kwon, M.; Park, J.; Bae, W. K.; Lee, S. W.; Cho, J. High-power Hybrid Biofuel Cells Using Layer-by-Layer Assembled Glucose Oxidase-Coated Metallic Cotton Fibers. *Nat. Commun.* **2018**, *9*, 1−11.
(18) Mano, N.; De Poulpiquet, A. O_2 Reduction in Enzymatic Biofuel Cells. *Chem. Rev. (Washington, DC, U. S.)* **2018**, *118*, 2392−2468.
(19) Baughman, R. H.; Zakhidov, A. A.; de Heer, W. A. Carbon Nanotubes–the Route Toward Applications. *Science* **2002**, *297*, 787−792.
(20) Chen, W.; Cai, S.; Ren, Q. Q.; Wen, W.; Zhao, Y. D. Recent Advances in Electrochemical Sensing for Hydrogen Peroxide: A Review. *Analyst (Cambridge, U. K.)* **2012**, *137*, 49−58.
(21) Kyaw, A. K. K.; Tantang, H.; Wu, T.; Ke, L.; Peh, C.; Huang, Z. H.; Zeng, X. T.; Demir, H. V.; Zhang, Q.; Sun, X. W. Dye-sensitized Solar Cell with a Titanium-oxide-modified Carbon Nanotube Transparent Electrode. *Appl. Phys. Lett.* **2011**, *99*, No. 021107(1)-021107(3).
(22) Kwon, C. H.; Ko, Y.; Shin, D.; Lee, S. W.; Cho, J. Highly Conductive Electrocatalytic Metal Nanoparticle-Assembled Carbon Fiber Electrodes for High-Performance Glucose-Based Biofuel Cells. *J. Mater. Chem. A* **2019**, *7*, 13495−13505.
(23) Guiseppi-Elie, A.; Lei, C.; Baughman, R. H. Direct Electron Transfer of Glucose Oxidase on Carbon Nanotubes. *Nanotechnology* **2002**, *13*, 559−564.
(24) Zebda, A.; Gondran, C.; Le Goff, A.; Holzinger, M.; Cinquin, P.; Cosnier, S. Mediatorless High-Power Glucose Biofuel Cells Based on Compressed Carbon Nanotube-Enzyme Electrodes. *Nat. Commun.* **2011**, *2*, 370−376.
(25) Weber, J.; Kumar, A.; Kumar, A.; Bhansali, S. Novel Lactate and PH Biosensor for Skin and Sweat Analysis Based on Single Walled Carbon Nanotubes. *Sens. Actuators, B* **2006**, *117*, 308−313.
(26) María D, R.; Gustavo A, R. Enzymatic Biosensors Based on Carbon Nanotubes Paste Electrodes. *Electroanalysis* **2005**, *17*, 73−78.
(27) Shim, M.; ShiKam, N. W.; Chen, R. J.; Li, Y.; Dai, H. Functionalization of Carbon Nanotubes for Biocompatibility and Biomolecular Recognition. *Nano Lett.* **2002**, *2*, 285−288.
(28) Besteman, K.; Lee, J. O.; Wiertz, F. G. M.; Heering, H. A.; Dekker, C. Enzyme-Coated Carbon Nanotubes as Single-Molecule Biosensors. *Nano Lett.* **2003**, *3*, 727−730.
(29) Smart, S. K.; Cassady, A. I.; Lu, G. Q.; Martin, D. J. The Biocompatibility of Carbon Nanotubes. *Carbon* **2006**, *44*, 1034−1047.
(30) Reid, R. C.; Minteer, S. D.; Gale, B. K. Contact Lens Biofuel Cell Tested in a Synthetic Tear Solution. *Biosens. Bioelectron.* **2015**, *68*, 142−148.
(31) Lee, J. Y.; Shin, H. Y.; Lee, J. H.; Song, Y. S.; Kang, S. W.; Park, C.; Kim, J. B.; Kim, S. W. A Novel Enzyme-Immobilization Method for a Biofuel Cell. *J. Mol. Catal. B: Enzym.* **2009**, *59*, 274−278.
(32) Higgins, S. R.; Lau, C.; Atanassov, P.; Minteer, S. D.; Cooney, M. J. Hybrid Biofuel Cell: Microbial Fuel Cell with an Enzymatic Air-Breathing Cathode. *ACS Catal.* **2011**, *1*, 994−997.
(33) Morozan, A.; Jousselme, B.; Palacin, S. Low-Platinum and Platinum-Free Catalysts for the Oxygen Reduction Reaction at Fuel Cell Cathodes. *Energy Environ. Sci.* **2011**, *4*, 1238−1254.
(34) Lin, L.; Zhu, Q.; Xu, A. W. Noble-Metal-Free Fe−N/C Catalyst for Highly Efficient Oxygen Reduction Reaction under Both Alkaline and Acidic Conditions. *J. Am. Chem. Soc.* **2014**, *136*, 11027−11033.
(35) Gokhale, R.; Chen, Y.; Serov, A.; Artyushkova, K.; Atanassov, P. Novel Dual Templating Approach for Preparation of Highly Active Fe-N-C Electrocatalyst for Oxygen Reduction. *Electrochim. Acta* **2017**, *224*, 49−55.
(36) Stariha, S.; Artyushkova, K.; Workman, M. J.; Serov, A.; Mckinney, S.; Halevi, B.; Atanassov, P. PGM-Free Fe-N-C Catalysts for Oxygen Reduction Reaction: Catalyst Layer Design. *J. Power Sources* **2016**, *326*, 43−49.
(37) Gajda, I.; Greenman, J.; Santoro, C.; Serov, A.; Melhuish, C.; Atanassov, P.; Ieropoulos, I. A. Improved Power and Long Term Performance of Microbial Fuel Cell with Fe-N-C Catalyst in Air-Breathing Cathode. *Energy* **2018**, *144*, 1073−1079.
(38) Sebastián, D.; Serov, A.; Matanovic, I.; Artyushkova, K.; Atanassov, P.; Aricò, A. S.; Baglio, V. Insights on the Extraordinary Tolerance to Alcohols of Fe-N-C Cathode Catalysts in Highly Performing Direct Alcohol Fuel Cells. *Nano Energy* **2017**, *34*, 195−204.
(39) Zhang, G.; Chenitz, R.; Lefèvre, M.; Sun, S.; Dodelet, J. P. Is Iron Involved in the Lack of Stability of Fe/N/C Electrocatalysts Used to Reduce Oxygen at the Cathode of PEM Fuel Cells? *Nano Energy* **2016**, *29*, 111−125.
(40) Wei, Q.; Zhang, G.; Yang, X.; Chenitz, R.; Banham, D.; Yang, L.; Ye, S.; Knights, S.; Sun, S. 3D Porous Fe/N/C Spherical Nanostructures As High-Performance Electrocatalysts for Oxygen Reduction in Both Alkaline and Acidic Media. *ACS Appl. Mater. Interfaces* **2017**, *9*, 36944−36954.
(41) Tan, S. L. J.; Kan, J. M.; Webster, R. D. Differences in Proton-Coupled Electron-Transfer Reactions of Flavin Mononucleotide (FMN) and Flavin Adenine Dinucleotide (FAD) between Buffered and Unbuffered Aqueous Solutions. *J. Phys. Chem. B* **2013**, *117*, 13755−13766.

DOI: 10.1021/acsami.9b14486
ACS Appl. Mater. Interfaces 2019, 11, 42744−42750

(42) Laviron, E. General Expression of the Linear Potential Sweep Voltammogram in the Case of Diffusionless Electrochemical Systems. *J. Electroanal. Chem. Interfacial Electrochem.* **1979**, *101*, 19−28.
(43) Eckermann, A. L.; Feld, D. J.; Shaw, J. A.; Meade, T. J. Electrochemistry of Redox-Active Self-Assembled Monolayers. *Coord. Chem. Rev.* **2010**, *254*, 1769−1802.
(44) Wu, M. Y.; Wang, J.; Li, H.; Zheng, J. G.; Wu, N. N. A Lactate Electrochemical Biosensor with a Titanate Nanotube as Direct Electron Transfer Promoter. *Nanotechnology* **2008**, *19*, No. 0755029(1)-0755029(6).
(45) Parra, A.; Casero, E.; Vázquez, L.; Pariente, F.; Lorenzo, E. Design and Characterization of a Lactate Biosensor Based on Immobilized Lactate Oxidase onto Gold Surfaces. *Anal. Chim. Acta* **2006**, *555*, 308−315.
(46) Romero, M. R.; Ahumada, F.; Garay, F.; Baruzzi, A. M. Amperometric Biosensor for Direct Blood Lactate Detection. *Anal. Chem.* **2010**, *82*, 5568−5572.
(47) Guler, M.; Turkoglu, V.; Basi, Z. Determination of Malation, Methidathion, and Chlorpyrifos Ethyl Pesticides Using Acetylcholinesterase Biosensor Based on Nafion/Ag@rGO-NH_2 Nanocomposites. *Electrochim. Acta* **2017**, *240*, 129−135.
(48) Gamero, M.; Pariente, F.; Lorenzo, E.; Alonso, C. Nanostructured Rough Gold Electrodes for the Development of Lactate Oxidase-Based Biosensors. *Biosens. Bioelectron.* **2010**, *25*, 2038−2044.

DOI: 10.1021/acsami.9b14486
ACS Appl. Mater. Interfaces 2019, 11, 42744−42750